PARTICLE TRACKING SIMULATION WITH SPACE CHARGE EFFECTS FOR AN INDUCTION SYNCHROTRON AND PRELIMINARY APPLICATION TO THE KEK DIGITAL ACCELERATOR

X. Liu#
Tokyo Institute of Technology, Nagatsuda, Kanagawa, Japan
High Energy Accelerator Research Organization (KEK), Tsukuba, Ibaraki, Japan

Abstract

In order to study the beam behaviour of the induction synchrotron which features low energy injection, a dedicated particle tracking simulation code with a 2.5D space charge field solver, which takes into account of the boundary condition, has been developed. The beam dynamics included in this code are discussed and simulation results assuming parameters of the KEK Digital Accelerator are presented. This code will help to understand the various features of the beam behaviour in the present beam commissioning and serve as a tool for the design of the future induction synchrotrons.

INTRODUCTION

The concept of induction synchrotron has been raised around 2000 by K. Takayama and J. Kishiro [1]. This concept has been experimentally confirmed in 2006 with the former KEK Proton Synchrotron (PS) [2]. After that, the booster for the KEK-PS has been modified to the present KEK Digital Accelerator [3]. The beam commissioning has been started since the middle of 2011 and the recent experimental studies can be seen in [4] and [5]. Though the longitudinal motion has been discussed in [6] and the longitudinal space charge field has been studied with simulation in [7], the 3D particle tracking simulation with the space charge has not been done yet.

In this paper, a 2.5D "slice-by-slice" scheme and the space charge solver with a boundary matrix method will be discussed. The justification of this solver is also described. Preliminary results of its application to the KEK-DA will be briefly shown.

SCHEME DESIGN

The following vector is chosen to represent the information of a macro particle in the simulation:

$$\vec{x} = (x, xp, y, yp, z, dpp) \tag{1}$$

where (x, xp) and (y, yp) are the positions in the horizontal and vertical phase space respectively, and $(z, \Delta p/p)$ is the longitudinal phase space. Here $z = s - \beta_0 c \cdot dt$ ($\beta_0 = v_0 / c$, v_0 is the velocity of the reference particle and c is the light speed) is the particle's longitudinal distance and $\Delta p / p$ is the momentum deviation from the referential particle.

For particle tracking without the space charge from s_0 to s_1 along the beam orbit of the referential particle, the change of particle information defined in Eq. (1) is given by,

$$\vec{x}_{s_1} = M_{s_0 \to s_1} \cdot \vec{x}_{s_0} \tag{2}$$

where M is a 6×6 transfer matrix from s_0 to s_1. In order to include the space charge and keep the simplicity of Eq. (2), the single kick approximation is used [8],

$$x(s) \xrightarrow{K_{sc}} x(s)' \xrightarrow{M} x(s + \Delta s) \tag{3}$$

where K_{sc} is the kick due to space charge forces and $\Delta s = s_2 - s_1$. K_{sc} can be expressed with the space charge induced field [9]

$$\vec{x}_{sc} = (0, \frac{\Delta s \cdot Qe}{\gamma_0^2 p_0 \beta_0 c} E_x, 0, \frac{\Delta s \cdot Qe}{\gamma_0^2 p_0 \beta_0 c} E_y, 0, \frac{\Delta s \cdot Qe}{\beta_0^2 E_{total}} E_z) \tag{4}$$

Here we assume that during a very small step size of Δs , the change of the space charge field caused from a change of the beam distribution is ignorable. In Eq.(4), (E_x, E_y, E_z) is the electric field in the beam frame, Q is the charge state of the particle, e is the unit electron charge, $\gamma_0 = 1/\sqrt{1-\beta_0^2}$, p_0 is the momentum and E_{total} is the total energy of the reference particle. The magnetic field due to moving beam is considered by including $1/\gamma_0^2$.

2.5D SPACE CHARGE SOLVER

A "slice-by-slice" scheme is chosen to solve the space charge field induced by the beam. In this scheme, the particle distribution will be longitudinally divided into k slices as seen in Fig. 1. Each slice will be meshed into $m \times n$ grids. Thus, there will be $m \times n \times k$ boxes in the 3D space.

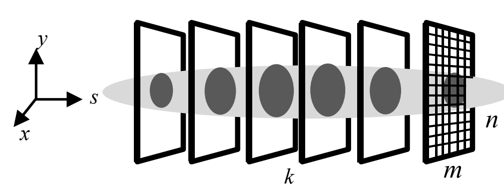

Figure 1: 2.5D slice-by-slice scheme.

The charge of the macro particles will be assigned to closest grid points (eight points for each macro particle) with the Particle-In-Cell (PIC) method, in which the

#liuxg@post.kek.jp

ISBN 978-3-95450-131-1

distances from the particle's position to the grid points are treated as weighting coefficients.

Then for each slice the transverse electric potential will be solved in a 2D manner. The transverse electric field is obtained from the potential. The longitudinal electric field is directly derived from the potential difference between adjacent slices.

Finite Method to Solve Poisson's Equation

Poisson's equation is,

$$\nabla\phi = -\frac{\rho}{\varepsilon_0} \tag{5}$$

where ϕ is the potential induced by the particle distribution, ρ is the charge density and ε_0 is the electric constant in vaccum.

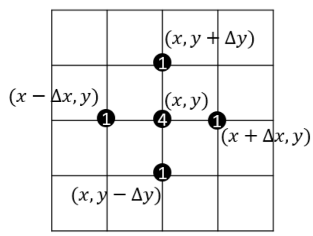

Figure 2: Finite method for Poisson's equation.

A finite method to solve this equation numerically is shown in Fig. 2, where the space is meshed into small tiles. In the case of $\Delta x = \Delta y = \Delta$, Eq. (5) in 2D case can be expressed as,

$$\phi(\Delta + x, y) + \phi(x, \Delta + y) - 4\phi(x, y) + \phi(x - \Delta, y) + \phi(x, y - \Delta) = -\frac{\rho(x, y)}{\varepsilon_0}\Delta^2 \tag{6}$$

Boundary Matrix Method

If the equations similar to Eq. (6) are written down for all points on the mesh, these equations will form a linear system with the left hand side (l.h.s) to be the potential on each grid point and the right hand side (r.h.s) to be the charge density, as shown below,

$$\begin{pmatrix} -4 & 1 & & & 1 & & & & \\ 1 & -4 & 1 & & & 1 & & \cdots & \\ & 1 & -4 & 1 & & & 1 & & \\ & & 1 & -4 & & & & 1 & \\ & \vdots & & & \ddots & & & \vdots & \\ & & & & & & -4 & 1 & \\ & & & & & & 1 & -4 & 1 \\ & \cdots & & & \cdots & & & 1 & -4 & 1 \\ & & & & & & & & 1 & -4 \end{pmatrix} \begin{pmatrix} \phi_1 \\ \phi_2 \\ \\ \\ \vdots \\ \\ \\ \phi_{n-1} \\ \phi_n \end{pmatrix}$$

$$= \begin{pmatrix} \rho_1 & \rho_2 & \cdots & \rho_n \end{pmatrix}^T \cdot \frac{\Delta^2}{\varepsilon_0} \tag{7}$$

Once the distribution is determined, the electrical potential can be obtained directly by solving Eq.(7), which can be easily solved with available numerical libraries such as Intel MKL[10] used in this simulation code.

The advantages of this method are obvious: (1) the boundary matrix determined only by the boundary shape, which allows any shape just by setting the potential of the grid points outside or on the boundary to be zero; (2) the number of boundary shape for accelerator is not so large, these boundary shapes can be prepared at the beginning and repeatedly used later.

Justification

In order to justify the method described in the previous subsection, two ideal distributions that the space charge potential and electric field can be obtained analytically have been considered.

The case of a round beam with current I_b in a cylindrical vacuum chamber is assumed as in Fig. 3. In the transverse direction, the beam is uniformly distributed within the beam radius a. The radius of the vacuum chamber is b.

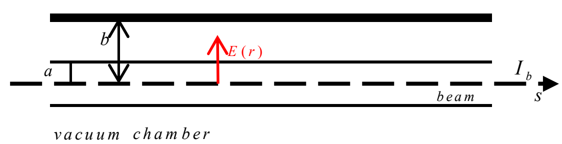

Figure 3: Round beam in cylindrical vacuum chamber.

The potential in the transverse direction with a distance r from the center of the beam can be obtained as,

$$E[r] = \begin{cases} \dfrac{\lambda}{2\pi\varepsilon_0}\dfrac{r}{a^2}, 0 \le r \le a \\ \dfrac{\lambda}{2\pi\varepsilon_0}\dfrac{1}{r}, a \le r \le b \end{cases} \tag{8}$$

where λ is the charge line density, related to the beam current I_b as,

$$\lambda = \frac{I_b}{\beta c} \tag{9}$$

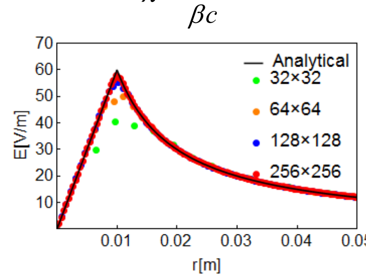

Figure 4: Simulation results compared with analytical solution.

Figure 4 shows the comparison between the simulation results and the analytical solution given by Eq. (8) where I_b =100 μA, $a = 1$ cm, $b = 10$ cm and β =0.01. In the simulation 10^4 number of macro particles are generated uniformly within the radius of a. In order to minimize the error for the field calculation, a large mesh size is often preferred, as shown in this figure.

ISBN 978-3-95450-131-1

In the case of a Gaussian distribution which has no sharp edge in the beam distribution, the electric field is given by

$$E[r] = \frac{1 - e^{-r^2/(2\sigma^2)}}{2\pi r \varepsilon_0} \lambda \tag{10}$$

where σ is the standard deviation for normal distribution. Similarly, the comparison between the simulation results and the analytical solution given by Eq. (10) is shown in Fig. 5 ($\sigma = a$), from which one can see that the result of 64×64 is better than that in Fig. 4 due to smooth beam distribution.

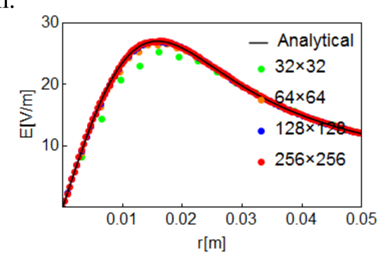

Figure 5: Simulation results for normal distribution.

PRELIMINARY APPLICATION TO THE KEK-DA

Lattice Calculation

With the guiding magnet components in the KEK-DA ring, the lattice functions can be calculated with this simulation code as shown in Fig. 6.

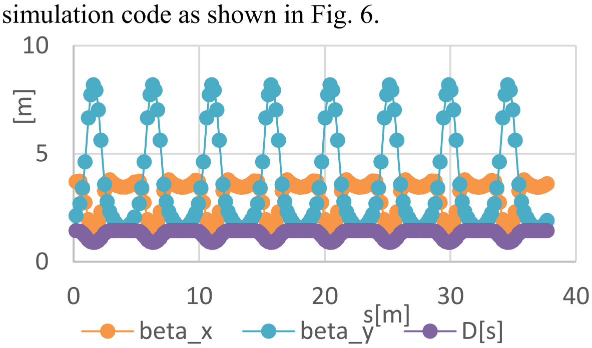

Figure 6: Lattice calculated for the KEK-DA ring.

Simulation Parameters Optimization

To minimize the error induced in the tracking simulation, the step size Δs has to be optimized. Figure 7 shows the rms emittance of a beam with transverse normal distribution is tracked one turn in the KEK-DA ring with different step size. It indicates that Δs should be less than 0.3m in this case.

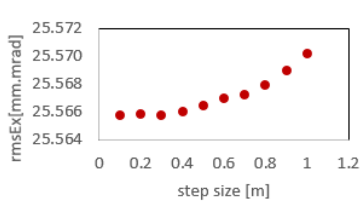

Figure 7: Step size optimization.

Static Magnetic Tracking Results

With the optimized step size, the beam can be tracked through the KEK-DA ring repeatedly to study the beam evolution due to the space charge force. For example, Fig. 8 shows transverse phase space of mismatched beam injection. In this simulation, the beam has the normal distribution in the transverse direction. The result shows that the beam tends to match the lattice and the evolution on the phase space due the space charge force.

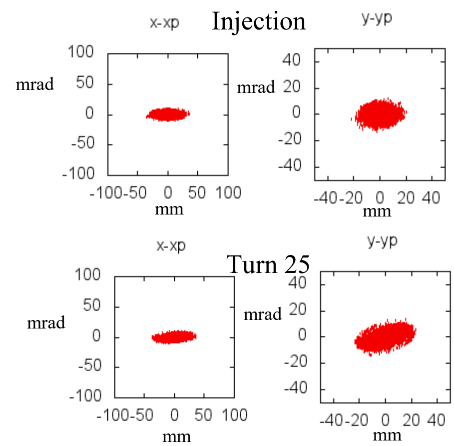

Figure 8: Phase space evolution of a mismatched beam.

CONCLUSION

A general simulation code considering the space charge with boundary conditions has been developed for the induction synchrotron. A 2.5D "slice-by-slice" scheme has been used and the boundary matrix method used as space charge solver has been well justified. Preliminary application to the KEK-DA, which is a fast cycling induction synchrotron, has been presented. Further study with the simulation to understand the beam behaviour in the KEK-DA ring will be continued and this simulation code can also be applied to the design and study of the future induction synchrotrons.

REFERENCES

[1] K. Takayama & J. Kishiro, Nucl. Instruments Methods Phys. Res. Sect. A. 451 (2000) 304–317.
[2] K. Takayama, et al., Phys. Rev. Lett. 98 (2007) 8–11.
[3] T. Iwashita, et al. , Phys. Rev. Spec. Top. - Accel. Beams. 14 (2011).
[4] X. Liu, et al., Laser Part. Beams. 33 (2015) 237–243.
[5] T. Yoshimoto, et al., Nucl. Instruments Methods Phys. Res. Sect. A 733 (2014) 141–146.
[6] T.S. Dixit, Nucl. Instruments Methods Phys. Res. Sect. A. 602 (2009) 326–336.
[7] X. Liu, et al. Proc. HIAT 2012. (2012) 83–88.
[8] A. Bazzani, et al., Cern Report (1994) 1–234.
[9] G. Franchetti, et al. Nucl. Instruments Methods Phys. Res. Sect. A. 415 (1998) 450–454.
[10] Intel, Intel ® Math Kernel Library, MKL 11.2, n.d.

ISBN 978-3-95450-131-1